Mechanistic Roles of Tyrosine 149 and Serine 124 in UDP-galactose 4-Epimerase from *Escherichia coli*†

Yijeng Liu, James B. Thoden, Jeongmin Kim, Elizabeth Berger, Andrew M. Gulick, Frank J. Ruzicka, Hazel M. Holden, and Perry A. Frey*

Institute for Enzyme Research, Graduate School, and Department of Biochemistry, College of Agricultural and Life Sciences, University of Wisconsin−Madison, Madison, Wisconsin 53705

Received February 25, 1997; Revised Manuscript Received June 17, 1997⊗

ABSTRACT: Synthesis and overexpression of a gene encoding *Escherichia coli* UDP-galactose 4-epimerase and engineered to facilitate cassette mutagenesis are described. General acid−base catalysis at the active site of this epimerase has been studied by kinetic and spectroscopic analysis of the wild-type enzyme and its specifically mutated forms Y149F, S124A, S124V, and S124T. The X-ray crystal structure of Y149F as its abortive complex with UDP-glucose is structurally similar to that of the corresponding wild-type complex, except for the absence of the phenolic oxygen of Tyr 149. The major effects of mutations are expressed in the values of k_{cat} and k_{cat}/K_m. The least active mutant is Y149F, for which the value of k_{cat} is 0.010% of that of the wild-type epimerase. The activity of S124A is also very low, with a k_{cat} value that is 0.035% of that of the native enzyme. The values of K_m for Y149F and S124A are 12 and 21% of that of the wild-type enzyme, respectively. The value of k_{cat} for S124T is about 30% of that of the wild-type enzyme, and the value of K_m is similar to that of the native enzyme. The reactivities of the mutants in UMP-dependent reductive inactivation by glucose are similarly affected, with k_{obs} being decreased by 6560-, 370-, and 3.4-fold for Y149F, S124A, and S124T, respectively. The second-order rate constants for reductive inactivation by $NaBH_3CN$, which does not require general base catalysis, are similar to that for the native enzyme in the cases of S124A, S124T, and S124V. However, Y149F reacts with $NaBH_3CN$ 12−20-fold faster than the wild-type enzyme at pH 8.5 and 7.0, respectively. The increased rate for Y149F is attributed to the weakened charge-transfer interaction between Phe 149 and NAD^+, which is present with Tyr 149 in the wild-type enzyme. The charge-transfer band is present in the serine mutants, and its intensity at 320 nm is pH-dependent. The pH dependencies of A_{320} showed that the pK_a values for Tyr 149 are 6.08 for the wild-type epimerase, 6.71 for S124A, 6.86 for S124V, and 6.28 for S124T. The low pK_a value for Tyr 149 is attributed mainly to the positive electrostatic field created by NAD^+ and Lys 153 (4.5 kcal mol^{-1}) and partly to hydrogen bonding with Ser 124 (1 kcal mol^{-1}). The pK_a of Tyr 149 is the same as the kinetic pK_a for the Bronsted base that facilitates hydride transfer to NAD^+. We concluded that Tyr 149 provides the driving force for general acid−base catalysis, with Ser 124 playing an important role in mediating proton transfer.

UDP-galactose 4-epimerase (epimerase) catalyzes the interconversion of UDP-Gal[1] and UDP-Glc, a step in the metabolism of galactose. In preceding steps of galactose catabolism, galactokinase catalyzes the phosporylation of α-D-galactose to galactose-1-P by ATP, and galactose-1-P uridylyltransferase catalyzes the reaction of UDP-glucose with galactose-1-P to produce UDP-Gal and glucose-1-P, which enters the glycolytic pathway. The epimerase regenerates UDP-Glc from UDP-Gal, thereby maintaining the production of glucose-1-P. Epimerase contains NAD^+ as the tightly bound coenzyme and is a member of the superfamily of proteins known as the short-chain dehydrogenases/reductases (*1*−*3*). This family includes mammalian 3β-hydroxysteroid dehydrogenase, plant dihydroflavonol reductase, Nocardia cholesterol dehydrogenase, 3α,20β-hydroxysteroid dehydrogenase, dihydropteridine reductase, and 7α-hydroxysteroid dehydrogenase from *Escherichia coli.* High-resolution X-ray crystal structures of epimerase, dihydropteridine reductase, 7α-hydroxysteroid dehydrogenase, mouse lung carbonyl reductase, 17β-hydroxysteroid dehydrogenase, and 3α,20β-hydroxysteroid dehydrogenase reveal similarities in the three-dimensional structures of these enzymes (*4*−*14*).

The current working hypothesis for the mechanism of nonstereospecific hydride transfer by epimerase is illustrated in Scheme 1. The binding of UDP-Gal to the enzyme induces a conformational change in the protein (**E***) that enhances the reactivity of NAD^+ as a hydride acceptor. Transfer of the C4-hydrogen and two electrons from UDP-Gal to the nicotinamide 4-*pro-S* position of NADH produces

† This work was supported by Grants GM30840 (P.A.F.) and GM15950 (J.B.T.) from the National Institute of General Medical Sciences and Grant DK47814 (H.M.H) from the National Institute of Diabetes and Digestive and Kidney Diseases, USPHS.

⊗ Abstract published in *Advance ACS Abstracts,* August 15, 1997.

[1] Abbreviations: dNTP, 2′-deoxynucleoside triphosphate; NAD^+, nicotinamide adenine dinucleotide; NADH, reduced NAD^+; UDP-Glc, uridine 5′-diphosphate glucose; UDP-Gal, uridine 5′-diphosphate galactose; UDP-6-Glc, UDP-glucose with glucose attached to UDP through its 6-hydroxyl group; UDP-phenol, uridine 5′-diphosphate phenol; galactose-1-P, α-D-galactose 1-phosphate; glucose-1-P, α-D-glucose 1-phosphate; ADPR, adenosine 5′-diphosphate ribose; Y149F, epimerase mutant with Tyr 149 changed to Phe; S124A, epimerase mutant with Ser 124 changed to Ala; S124T, epimerase mutant with Ser 124 changed to Thr; S124V, epimerase mutant with Ser 124 changed to Val; Tris, tris(hydroxymethyl)aminomethane; CHES, 2-(*N*-cyclohexylamino)ethanesulfonate; EDTA, ethylenediaminetetraacetic acid; PCR, polymerase chain reaction; bp, base pair.

S0006-2960(97)00430-3 CCC: $14.00

Scheme 1

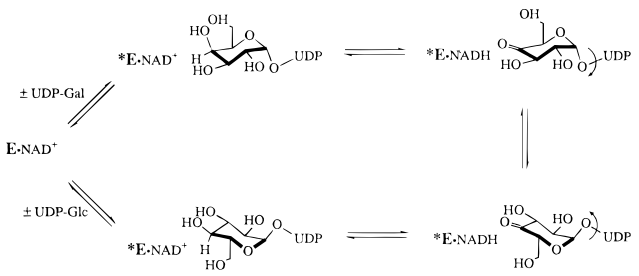

UDP-4-ketoglucopyranoside at the active site. A conformational change in the keto intermediate, mainly by rotational reorientation about the bond linking the anomeric oxygen to P_β of UDP, allows the opposite face of the 4-keto group to approach NADH and accept the hydrogen and two electrons from the 4-*pro-S* position of NADH, thus forming UDP-Glc and NAD^+. A substantial body of kinetic, stereochemical, and binding information inspired the formulation of this mechanism (*15*), and it has recently received structural support as well (*16*).

The active site of epimerase contains three amino acids that appear to function in important ways in the catalytic process, Lys 153, Tyr 149, and Ser 124 (*5*, *17*). The other members of the superfamily also contain the Lys and Tyr residues at corresponding amino acid sequence and three-dimensional structural positions, and most of them retain the Ser residue as well, although dihydropteridine reductase does not contain a residue corresponding to Ser 124. Epimerase differs from the other members of the superfamily in that NAD^+ is very tightly bound and functions as a coenzyme rather than as a substrate. Tight binding of NAD^+ to epimerase appears to arise through a large number of main chain and side chain hydrogen-bonded contacts with the adenosyl portion of the coenzyme (*4*).

All crystal structural models of epimerase show that Lys 153 is hydrogen-bonded to the hydroxyl groups of the nicotinamide riboside portion of NAD^+ (*4*−*6*), and it also plays an important part in the uridine nucleotide-induced conformational change that enhances the chemical reactivity of NAD^+ (*17*). The structure of a stable, abortive complex consisting of epimerase to which NADH and UDP-Glc are tightly bound (E·NADH·UDP-Glc) shows that the phenol ring of Tyr 149 is placed near the nicotinamide ring of NAD^+, Ser 124, and the 3-OH group of the glucosyl ring, with the hydroxyl group of Ser 124 being hydrogen-bonded to the 4-OH group of the glucosyl ring (*5*). The structure in this region of the abortive complex implicates Tyr 149 and Ser 124 in the interactions between the glucosyl group of UDP-Glc and NAD^+, most likely in the chemistry of the epimerization process.

In this paper, we describe the synthesis of an engineered version of the epimerase gene designed for use in cassette mutagenesis. We present the kinetic, chemical, and spectrophotometric properties of specific mutated versions of epimerase, including Y149F, S124A, S124T, and S124V. We also compare the X-ray crystal structure of Y149F with that of the wild-type epimerase.

EXPERIMENTAL PROCEDURES

Materials. Restriction endonucleases were purchased from Boehringer Mannheim or United States Biochemicals and used according to the manufacturer's recommendations. T4 polynucleotide kinase, T4 DNA ligase, and calf intestine phosphatase were from Boerhinger Mannheim. Taq polymerase was obtained from Epicentre Technologies (Madison, WI). [^{35}S]dATP$_\alpha$S (600 Ci/mmol) was from Amersham. β-Cyanoethyl diisopropylamino phosphoramidites, long-chain alkylamine controlled pore glass, and all other reagents for oligodeoxynucleotide synthesis were from Biosearch or Glen Research. Oligonucleotides used in cassette mutagenesis were purchased from commercial vendors. The bacterial strains and plasmids were purchased from United States Biochemicals.

Cloning vector pTZ19RB was prepared by modifying pTZ19R so as to replace the *Hinc*II restriction site with a *Bss*HII site, in order to clone the synthetic duplex BK (Figure 1) into the vector. This was done by replacing the region between the *Pst*I and *Xba*I sites in pTZ19R with a synthetic duplex that replaced the *Hinc*II site with the sequence corresponding to the *Bss*HII site.

Methods. UDP-galactose 4-epimerase and site-specific mutants were expressed in *E. coli* BL21 cells and purified as described (*17*, *18*). One unit of enzyme activity was defined as the amount of enzyme required to produce 1 μmol of UDP-Glc per minute under standard assay conditions (*19*). All preparations of purified, homogeneous epimerase contained significant amounts of the inactive, abortive complexes epimerase·NADH·uridine nucleotide (*18*). Therefore, samples were analyzed for abortive complexes by spectrophotometric analysis, and kinetic data were corrected for the presence of small amounts of these complexes (*19*). Kinetic measurements and spectrophotometric characterization of the charge transfer bands associated with epimerase and its mutated forms S124A, S124T, and S124V were carried out in a Hewlett-Packard 8452 diode array spectrophotometer. The mutant Y149F did not display a significant charge-transfer band.

Procedures for cloning DNA into plasmids were as described (*20*). The dideoxy sequencing method using denatured plasmid templates (*21*) was used with [^{35}S]dATP$_\alpha$S to sequence the entire gene after cloning into pTz19R. The universal and the reverse primers that hybridize to sequences near the multiple cloning sites in the plasmid pTz19R were used to sequence both ends of the gene. Sequencing of specific regions of the gene was facilitated by the use of appropriate primers from the pool of synthetic oligodeoxynucleotides.

Pseudo-first-order rate constants for UMP-dependent reduction of epimerase·NAD^+ and specific mutants by 1 M glucose were measured spectrophotometrically at 340 nm as functions of UMP concentration. The limiting rate constants k and K_m for UMP were determined by fitting data to the equation $k = k_{obs}[UMP]/([UMP] + K_m)$. Second-order rate constants for reduction of epimerase·NAD^+ and specific mutants by $NaBH_3CN$ were calculated from initial rates measured at 340 nm in the presence and absence of 5 mM UMP.

Synthesis of Oligodeoxynucleotides and Assembly into Gene Fragments HB, BK, and KE. Oligodeoxynucleotides H1−H10, B1−B10, and K1−K10 used in the assembly of the engineered epimerase gene (Figure 1) were synthesized by use of a Biosearch model 8600 DNA synthesizer. Standard procedures were employed to deprotect and cleave the oligomers from the solid support (*22*), and stepwise yields were 97−99% per cycle. Following electrophoresis on a

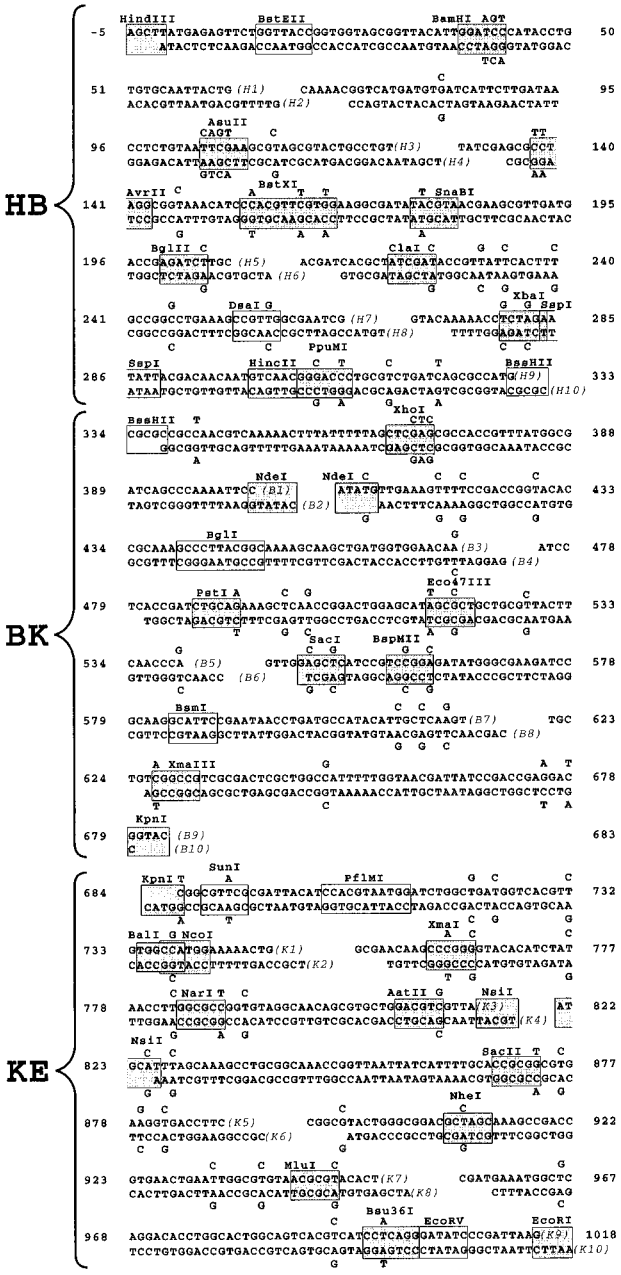

FIGURE 1: Design of an engineered gene for UDP-galactose 4-epimerase. Shown are the nucleotide sequences of oligonucleotides used for the synthesis of an engineered version of the gene specifying *E. coli* UDP-galactose 4-epimerase. The synthetic oligonucleotides are shown aligned in duplexes in the order of their appearance in the finished gene. The bases shown above and below the duplexes at selected positions are those that exist in the wild-type gene and were changed in the engineered gene. The complete synthetic gene was assembled in two major stages. Duplexes formed from oligonucleotides H1−H10 were hybridized and ligated to form the major gene fragment HB. Similarly, oligonucleotides B1−B10 were used to produce the gene fragment BK, and fragment KE was synthesized from oligonucleotides K1−K10. The major fragments were then amplified by PCR and ligated in the order shown to produce the finished synthetic gene. The shaded boxes indicate the newly created unique restriction sites, and the open boxes indicate the unique restriction sites that were retained from the wild-type gene.

12% polyacrylamide gel, oligonucleotides were purified as described (*23*). All oligodeoxynucleotides, except the two containing the external 5′ termini of the major gene fragments HB, BK, and KE (Figure 1), were phosphorylated at the 5′ ends (*24*). The hybridization reaction mixtures (30 μL) containing the complementary oligodeoxynucleotide duplexes for a given gene fragment, Tris-HCl at pH 7.6 (20 mM) and $MgC1_2$ (10 mM) were heated at 95 °C for 30 s, incubated at 65 °C for 20 min, and then cooled to room temperature for about 30 min. The ligation reaction mixtures (200 μL) contained five pairs of duplexes (50 pmol each) derived from the above reactions, Tris-HCl at pH 7.6 (20 mM), $MgCl_2$ (10 mM), ATP (1 mM), dithiothreitol (5 mM), and 10 units of T4 DNA ligase. Incubation was at 16 °C for 4 h. The assembled gene fragments HB, BK, and KE were purified by low-melting temperature agarose gel electrophoresis (25).

PCR Amplifications of Gene Fragments HB and KE and the Gene HE. Amplifications were carried out by the method of Saiki et al. (*26*) with the following modifications. Amplification reactions with Taq polymerase took place in 50 μL reaction mixtures containing 1 ng of duplex HB, KE, or HE (the assembled gene) in 67 mM Tris-HCl, 6.7 mM EDTA, 0.7 ng of each primer, each dNTP at 1 mM, and 1 unit of polymerase at pH 8.8 and 25 °C. The samples were overlaid with several drops of mineral oil to prevent evaporation and subjected to 20 cycles of the following amplification procedure. The samples were heated to 95 °C for 30 s, cooled to 60 °C, and incubated at that temperature for 5 min. Additional Taq polymerase was added to the samples after the tenth cycle.

Gene fragment BK was cloned into pTZ19RB for amplification of the DNA, whereas fragments HB and KE were amplified by PCR. Short extension primers were used for the PCR, and the ends of the PCR products were trimmed with the appropriate restriction endonucleases.

Final Assembly of the Engineered Gene for UDP-galactose 4-Epimerase. The PCR product from duplex HB, designated HB′, was restriction digested with *Bss*HII to duplex HB″, which was blunt on the 5′ end and sticky on the 3′ end. The duplex KE″ was similarly obtained by digestion of PCR product KE′ with the endonuclease *Kpn*I and had a sticky 5′ end and a blunt 3′ end. The duplex BK was excised at the flanking restriction sites from the plasmid pTZ19RBK. The full length gene was assembled in a ligation reaction containing each of the three duplexes HB″, BK, and KE″ and then amplified with Taq polymerase by use of the primers that had been employed in the amplification of duplexes HB (5′ end) and KE (3′ end). The amplified gene was digested by endonucleases *Hin*dIII and *Eco*RI, isolated on an electrophoretic gel of low-melting temperature agarose, and then cloned into the *Hin*dIII and *Eco*RI sites of pTZ19R. The nucleotide sequence of the whole gene was determined by using the universal and reverse primers for sequencing from double-stranded pTHE plasmid DNAs, as well as many of the synthetic oligodeoxynucleotides used in the synthesis of the duplexes.

Construction of a High-Expression Vector for the Synthetic Epimerase Gene. An overexpression vector containing the synthetic gene was constructed by insertion of the synthetic gene into the high-expression vector pT7E2 (*17*), which contained the wild-type gene derived from pI24 (*27*) together with the *gal* promoter and ribosome binding site behind the T7 promoter in pTZ18R. The combined effects of the T7 and *gal* promoters together with the ribosome binding site ensured high expression of epimerase. The vector pT7E2 was digested with *Bst*EII and *Pst*I, which removed all but 11 bp of the *gal*E gene downstream from the start codon to the multicloning site, and purified. The *Pst*I site was blunt-

Table 1: Intensity Statistics for Y149F·NADH·UDP-Glc

		resolution range (Å)							
	overall	30.0−3.80	3.02	2.63	2.39	2.22	2.09	1.99	1.90
no. of measurements	83309	13853	14800	10231	10051	9362	8763	8303	7941
no. of independent reflections	3546	4445	4270	4157	4176	4167	4149	4103	4050
completeness of data (%)	96	97	97	93	95	96	97	94	91
average intensity	3659	10000	6616	2394	1458	1156	944	701	533
average σ	196	267	222	149	146	167	181	190	200
R factor[a] (%)	3.9	2.4	3.8	6.6	9.1	11.0	13.6	16.7	20.7

[a] R factor $= (\sum|I-\bar{I}|/\sum I) \times 100$.

ended with T4 DNA polymerase and dNTPs. The vector pKFHE′ containing the synthetic epimerase gene was digested with *Eco*RI; the linearized DNA was blunt-ended with the Klenow fragment and dNTPs, purified by phenol extraction and ethanol precipitation, and partially digested with *Bst*EII to produce a 1010 bp insert, which was purified by low-melting temperature agarose gel electrophoresis. This insert, containing all but 11 bp of the synthetic gene, was ligated into the linearized plasmid obtained by *Bst*EII and *Pst*I digestion of pT7E2 to obtain the expression vector pTZsynE. The construct was first transformed into DH5α cells, and plasmid DNA obtained from them was used to transform BL21(DE3)pLysS cells for expression. The *Hin*dIII and *Eco*RI sites in the original synthetic gene (Figure 1) were sacrificed in the construction of this expression system.

Construction of the Mutant Plasmid Containing the Gene for Y149F. The plasmid containing the mutant gene encoding Y149F was constructed by cassette mutagenesis using the plasmid pTZSynE containing the synthetic gene. Mutagenesis was performed as described in the following paper (*28*). The codon for Tyr 149 was located within the five nonspecific bases of a *Bgl*I restriction site. Because multiple *Bgl*I restriction sites exist in the wild-type pTZSynE plasmid, it was digested briefly with *Bgl*I, and the linear 3835 bp fragments were purified from an agarose gel. The linear DNA was treated with T4 DNA polymerase to remove the 3′ overhang (*29*) which contained the Tyr 149 codon. The DNA was then cut with *Nde*I, and the resulting 3793 bp fragment was purified from an agarose gel and used as vector DNA, into which the Y149F cassette was inserted. The Y149F oligonucleotides (Y149F-top, ATATGTTGAAAGCTTTCCGACCGGTACACCGCAAAGCCCTTT; Y149F-bottom, AAAGGGCTTTGCGGTGTACCGGTCGGAAAGCTTTCAAC) contained a silent *Hin*dIII site to facilitate identification of the Y149F mutation. The plasmids were sequenced over the length of the mutagenic cassette.

X-ray Structural Determination. The Y149F epimerase was transformed into the abortive complex Y149F·NADH·UDP-Glc by reduction with the dimethylamine−borane complex as previously described (*5*). Large single crystals were grown by the hanging drop method of vapor diffusion against 20% poly(ethylene glycol) 8000, 600 mM NaCl, and 50 mM CHES buffer at pH 9.0 and 4 °C. The crystals belonged to the space group $P3_221$ with the following unit cell dimensions: $a = b = 83.8$ Å, $c = 107.8$ Å, and one subunit per asymmetric unit.

X-ray data were collected from a single crystal using a Siemens HI-STAR area detector system equipped with Supper Long double-focusing murrors. Prior to X-ray data collection, the crystal was flash-cooled to −150 °C in a nitrogen stream as previously described (*4*). The X-ray source was CuKα radiation from a Rigaku RU200 rotating anode generator operated at 50 kV and 90 mA and equipped with a 300 μm focal cup. The X-ray data were processed with the data reduction software package SAINT (Siemens Analytical X-ray Instruments) and internally scaled according to a procedure developed in the laboratory by G. Wesenberg. Relevant X-ray data collection statistics are given in Table 1.

Because the crystals of Y149F·NADH·UDP-Glc were isomorphous with respect to those previously described for the wild-type epimerase·NADH·UDP-Glc (*5*), the structure presented here was solved by difference Fourier techniques and refined by least-squares analysis with the program TNT to a resolution of 1.9 Å (*30*). The final R factor was 17.9% for all measured X-ray data between 30.0 and 1.9 Å with root-mean-square deviations from "ideal" geometry of 0.016 Å for bond lengths, 2.5° for bond angles, and 0.013 Å for trigonal planes. The model included 2705 protein atoms and 641 solvent molecules. The α-carbon atoms for the wild-type and mutant proteins were superimposed with a root-mean-square deviation of 0.08 Å.

RESULTS

Synthesis and Expression of an Engineered Gene for E. coli Epimerase. To facilitate the production of desired mutant forms of epimerase by cassette mutagenesis, the *E. coli* gene has been engineered to incorporate new, unique restriction sites at convenient locations throughout its length. The nucleotide sequences of the wild-type and engineered genes are shown in Figure 1 in the form of the sequences of oligonucleotide duplexes and of three gene fragments (HP, BK, and KE) from which the complete gene was assembled. The oligonucleotide duplexes were ligated by the action of DNA ligase to form the fragments HP, BK, and KE, respectively. The gene fragments were purified, amplified, and finally ligated into the full length gene. The gene was then excised from pTZ19RB and cloned into the over expression vector pT7E2, to produce pTZsynE (Figure 2) which contains the T7 and *gal* promoters in tandem ahead of a ribosome binding site and the epimerase start site. This vector expresses epimerase at very high levels in *E. coli.* Nucleotide sequence analysis of the ligated gene revealed a few mistakes that had been introduced by the PCR amplification of gene fragments and in the synthesis of one fragment. After correction of these mistakes by site-directed mutagenesis, using either the Kunkel method (*31*) or cassette mutagenesis, the epimerase was expressed from the synthetic gene in *E. coli* at levels approximately $^2/_3$ of that of the wild-type gene expressed by the same vector. Cells grown with

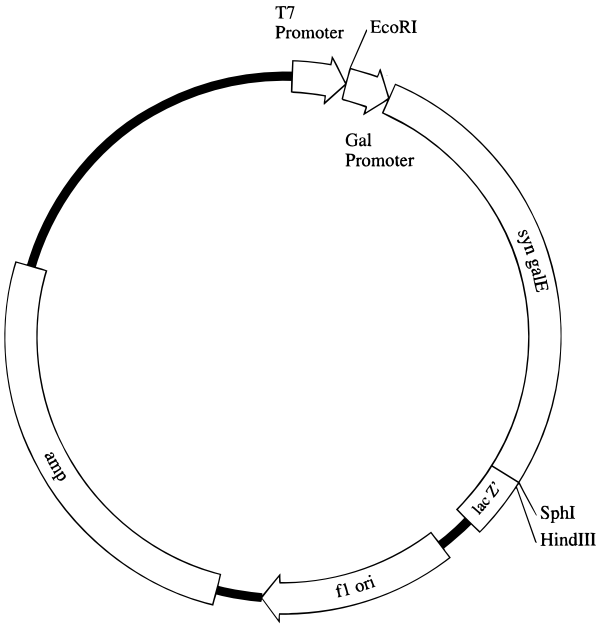

FIGURE 2: Vector for overexpression of the epimerase gene in *E. coli*.

this expression system produced epimerase and specific mutants at levels that allowed the purification of about 200 mg of enzyme from 50 g of packed cells.

Structural Similarity of Y149F with Wild-Type Epimerase. The crystal structures of the abortive complex forms of epimerase (epimerase·NADH·UDP-Glc) and Y149F show that the overall polypeptide chain folds are the same (Figure 3a). The structure of Y149F differs from that of the wild-type enzyme mainly in the absence of the hydroxyl group in the side chain of Tyr 149. The interactions among Tyr 149, Ser 124, NAD^+, and the glucosyl ring in the abortive complex are shown in Figure 3b. The hydroxyl group of Ser 124 is within 2.6 Å of the glucosyl 4-hydroxyl group (*5*). The phenolic oxygen of Tyr 149 is within hydrogen bonding distance of the 3-OH group of the glucosyl moiety (3.1 Å), and it is also near N-1 of the nicotinamide ring of NADH (3.6 Å), as well as within hydrogen bonding range of the 2'-hydroxyl group of the nicotinamide ribotide (2.9 Å). Both Ser 124 and Tyr 149 are in key positions that should allow them to participate in the oxidation/reduction mechanism.

Kinetic Properties of Y149F, S124A, S124T, and S124V. The kinetic parameters for catalysis of the overall transformation of UDP-Gal into UDP-Glc by the wild-type epimerase and the mutated forms Y149F, S124A, and S124T are given in Table 2. In general, the values of k_{cat} are much more sensitive than K_m to substitutions for Tyr 149 and Ser 124, although both are affected. Substitution of Phe for Tyr 149 severely impairs catalysis, decreasing k_{cat} to about 1/10000th of that of the wild-type epimerase. Mutation of Ser 124 to Ala also decreases k_{cat} to about 1/2900th of the value for wild-type epimerase, leaving S124A about 3.5 times as active as Y149F. Threonine at position 124 is functional, however, at about $^1/_3$ of the rate for serine. Although kinetic parameters are not available for S124V, its specific activity in the standard assay is 0.032 unit mg^{-1}, which is 0.008% of that of the wild-type enzyme (400 units mg^{-1}). The epimerase activity is compromised to a greater degree by the loss of the Tyr 149 phenolic oxygen than by the loss of the Ser 124 hydroxyl group; however, both are important.

To interpret the kinetic parameters in Table 2 for the mutant enzymes properly, consideration must be given to the possible effects of trace contamination by the wild-type epimerase. The mutant epimerases were expressed from plasmids in *E. coli* BL21 cells, which require galactose for growth. Whether the genetic lesion in BL21 cells prevents expression of the host epimerase gene was not known. Therefore, it was necessary to evaluate the mutant enzymes for wild-type contamination. The smaller values of K_m for Y149F and S124A relative to those of the wild-type epimerase indicated that the observed activities were not due to wild-type contamination. However, the following independent biochemical evidence proved that the activities recorded for the mutant enzymes in Table 2 could not be attributed to wild-type epimerase.

Epimerase is reductively inactivated by $NaBH_4$; however, reduction is sluggish in the absence of UMP and requires millimolar borohydride to go to completion. Moreover, although UMP stabilizes the epimerase·NADH complex, the NADH is reoxidized under aerobic conditions in the absence of UMP (*32*). The mutated enzyme Y149F differs, as shown in a later section, in that the associated NAD^+ is easily reduced by submillimolar concentrations of $NaBH_4$ and remains reduced under aerobic conditions in the absence of UMP, as determined spectrophotometrically and by activity measurements. The epimerase activity of the purified Y149F (60 μM subunits at pH 8.5 and 27 °C) is abolished within 10 min by 69 μM $NaBH_4$ and does not return within 24 h under aerobic conditions. The activity of wild-type epimerase (80 μM subunits at pH 8.5 and 25 °C) is decreased only 40% by 690 μM $NaBH_4$, and the enzyme is reactivated to its original activity after 1 h under aerobic conditions. Therefore, the effect of $NaBH_4$ on the epimerase activity of Y149F does not correspond to the wild-type enzyme. Furthermore, the pH dependence of the epimerase activity displayed by Y149F does not correspond to that of the wild-type enzyme, as shown in Figure 4. The break in the pH−rate profile on the acidic side for Y149F takes place at a much higher pH than that of the wild-type enzyme. If the epimerase activity of Y149F could be attributed to contamination by wild-type enzyme, it would display the wild-type pH dependence; therefore, the observed activity cannot be ascribed to wild-type contamination and must be assigned to the mutant.

Epimerase is subject to gradual inactivation at pHs lower than 6.0, and S124A is even less stable than the wild-type epimerase, as determined by activity measurements. At pH 5.5, the epimerase activity of the purified S124A is decreased by 70% within 40 min at 25 °C, whereas that of the wild-type enzyme decreases only 20% under the same conditions. If the epimerase activity of S124A were caused by wild-type contamination, it should display the same stability at pH 5.5. Because it cannot be ascribed to wild-type contamination, it can be assigned to the mutant. S124V is also more labile to low pHs than the wild-type enzyme.

Reactivities of Y149F, S124A, S124V, and S124T in UMP-Dependent Reductive Inactivation. Epimerase undergoes UMP-dependent reductive inactivation by reducing sugars, $NaBH_4$, and $NaBH_3CN$, and even by Tris buffer (*33*−*36*). In reductive inactivation, NAD^+ at the active site is reduced to NADH. The rate is greatly enhanced by UMP, which binds to the reduced enzyme to form a complex that is

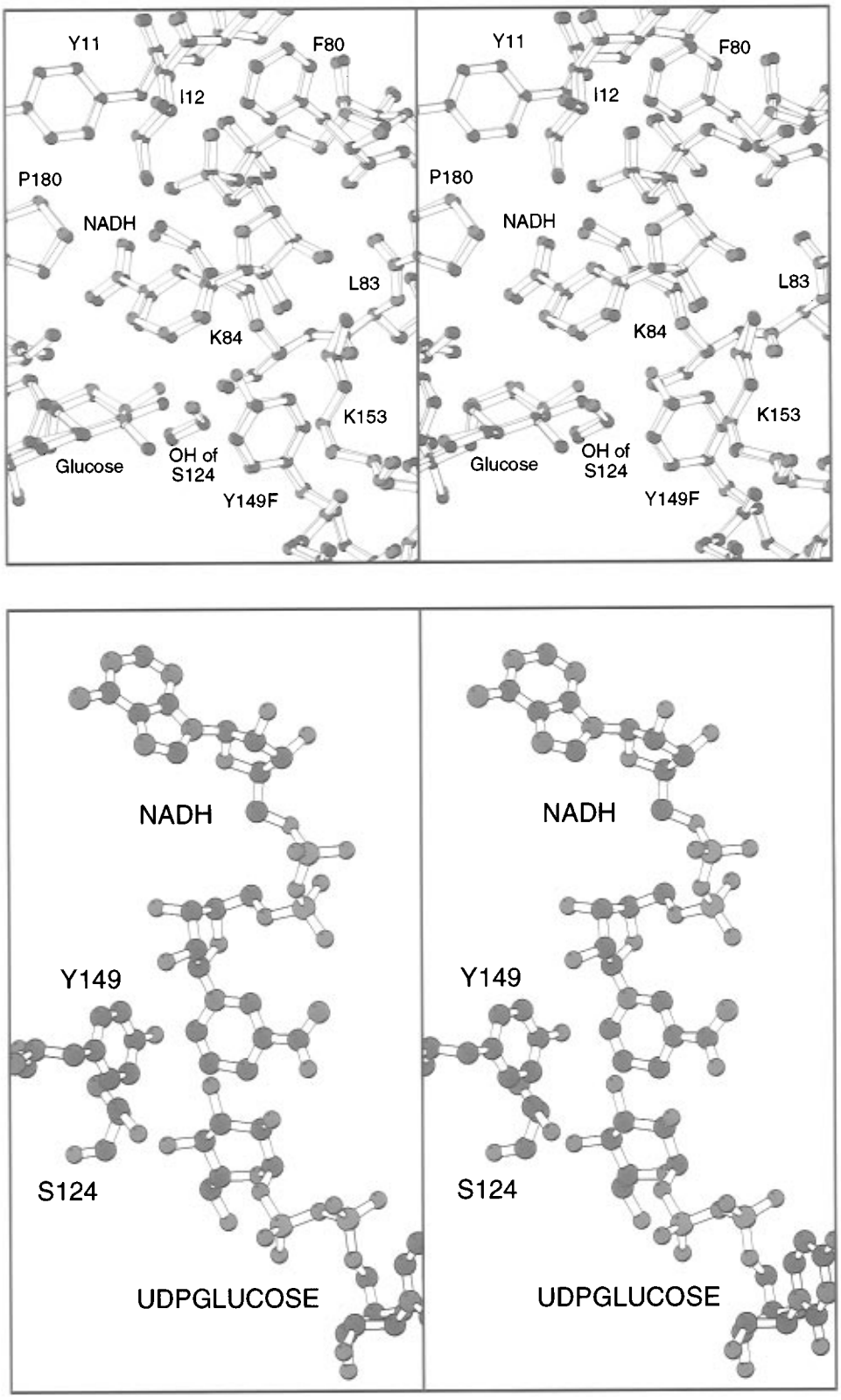

FIGURE 3: Structure of the abortive complex epimerase·NADH·UDP-Glc and the corresponding complex of Y149F. (a, top) An overlay of the abortive complexes in the active site region, including the nicotinamide ring of NAD^+ and the glucosyl ring of UDP-Glc. The wild-type enzyme is shown in red, with Y149F shown in black. Note the absence of the phenolic oxygen at position 149 in the structure of Y149F and the close structural correspondence in other respects. (b, bottom) The active site region of the wild-type abortive complex in closeup, showing the positions of Ser 124, Tyr 149, and the nicotinamide ring of NAD^+.

analogous to the abortive complex, with UMP in place of UDP-Glc. Rates for UMP-dependent reductive inactivation by glucose in Table 3 are expressed as pseudo-first-order rate constants at less than glucose saturation (1 M). Mutation of Tyr 149 to Phe decreases the rate to 1/6560th of that for wild-type epimerase. Mutation of Ser 124 to Ala also decreases the rate to 1/370th of the wild-type rate. Mutation of Ser 124 to Thr moderately decreases the rate to about 30% of the wild-type rate, showing that Thr can substitute for Ser 124 reasonably well, as in the overall reaction (Table 2).

Table 2: Kinetic Parameters for the Catalytic Activities of Epimerase and Specific Mutants[a]

epimerase	k_{cat} (s^{-1})	K_m (mM)	k_{cat}/K_m (s^{-1} mM^{-1})
wild-type	760 ± 11	0.225 ± 0.008	3380 ± 170
Y149F	0.073 ± 0.003	0.026 ± 0.004	2.85 ± 0.55
S124A	0.265 ± 0.004	0.048 ± 0.002	5.52 ± 0.31
S124T	248 ± 2	0.256 ± 0.005	967 ± 25

[a] Parameters were measured at pH 8.5 in 0.1 M sodium bicinate buffer at 27 °C.

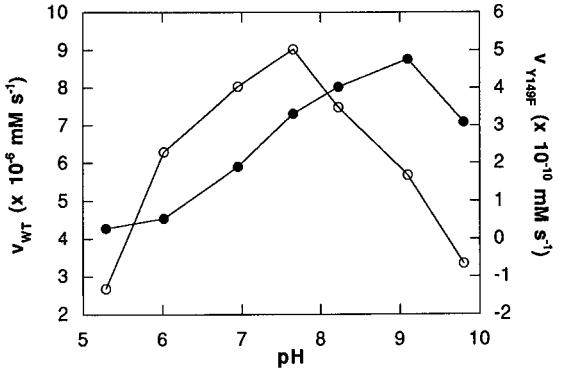

FIGURE 4: pH dependence of enzymatic activity for wild-type and Y149F epimerases. The initial rates for the transformation of UDP-galactose into UDP-glucose are plotted versus pH for wild-type epimerase and Y149F. Rates were measured at 27 °C at 0.05 mM UDP-galactose at various pHs from 5.5 to 10: (○) wild-type epimerase and (●) Y149F epimerase.

Table 3: Rates of UMP-Dependent Reductive Inactivation by Glucose[a]

epimerase	k_{obs} (min^{-1})	K_m^{UMP} (mM)
wild-type	4.75 ± 0.12	0.441 ± 0.042
Y149F	0.000724 ± 0.000038	0.394 ± 0.051
S124A	0.0129 ± 0.0003	0.115 ± 0.022
S124T	1.39 ± 0.03	0.564 ± 0.040

[a] Parameters were measured at 1 M Glc in 0.1 M KP_i buffer at pH 7.0 and 27 °C.

Table 4: Second-Order Rate Constants for Reductive Inactivation by $NaBH_3CN$

	$k \times 10^2$ (mM^{-1} min^{-1})			
	pH 8.5[a]		pH 7.0[b]	
epimerase	with UMP	without UMP	with UMP	without UMP
wild-type	1.45 ± 0.08	ND	16.6 ± 0.9	0.0248 ± 0.0023
Y149F	29 ± 2	0.96 ± 0.11	208 ± 13	3.32 ± 0.32
S124A	1.36 ± 0.07	ND	15.7 ± 1.0	0.098 ± 0.013
S124T	1.45 ± 0.11	ND	17.0 ± 1.5	0.0253 ± 0.0095
S124V	1.37 ± 0.27	ND	3.3 ± 0.9	0.0261 ± 0.0075

[a] Rates measured in 0.1 M sodium bicinate buffer at 27 °C. [b] Rates measured in 0.1 M KP_i buffer at 27 °C.

Rates of reductive inactivation by sodium cyanoborohydride are expressed in Table 4 as second-order rate constants. These rates are revealing on three planes. First, mutations at either Tyr 149 or Ser 124 do not significantly hamper reduction by sodium cyanoborohydride, which is a nonspecific reducing agent that would not require general base catalysis in hydride transfer to NAD^+. Second, mutation of Tyr 149 to Phe significantly *increases* the reduction rate, by 20-fold at pH 8.5 and 12-fold at pH 7.0. Given the fact that the main structural difference between the wild-type epimerase and Y149F is the absence of the phenolic oxygen in the mutant, it appears that the phenolic oxygen of Tyr 149

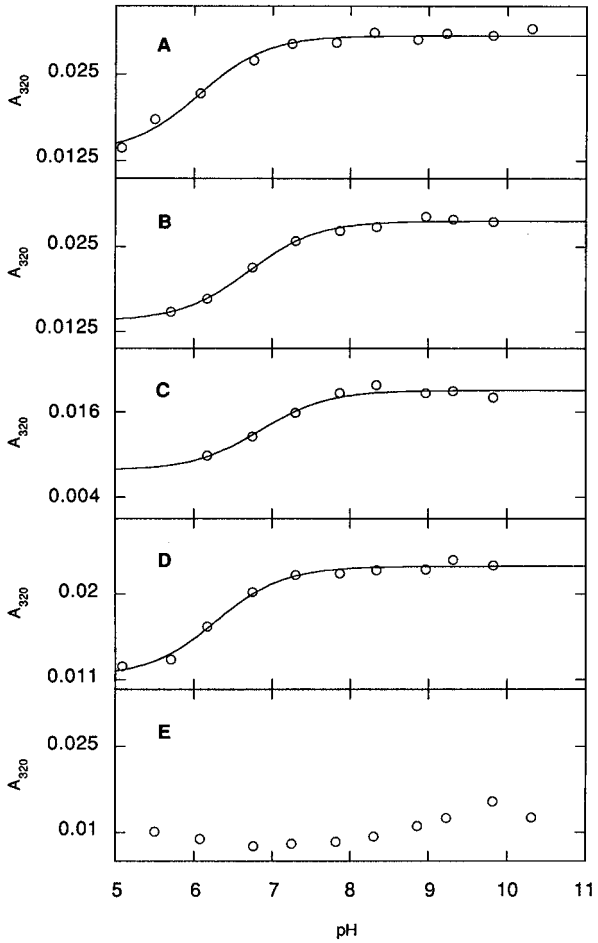

FIGURE 5: pH dependence of charge-transfer bands in free epimerase and active site mutants. Shown in parts A−D, respectively, are the variations with pH of the intensities of the charge-transfer bands in epimerase and its mutated forms S124A, S124V, and S124T. Part E shows comparable data on Y149F, which show that this mutant does not display the same charge-transfer band. The decreased charge transfer in this mutant implicates Tyr 149 in the charge-transfer interaction observed in the wild-type enzyme and serine mutants. The pH dependence of the charge transfer in the wild-type enzyme and serine mutants indicates that the phenolate of Tyr 149 is responsible for most of the charge-transfer band. The values of pK_a determined from the fitted curves are given in the text.

in the native enzyme attenuates the reactivity of NAD^+ toward $NaBH_3CN$. This will be attributed in the next section to charge-transfer complexation between Tyr 149 and NAD^+. Finally, UMP enhances the reduction rates of all epimerase mutants in Table 4, 126−670-fold in the cases of the wild type and Ser 124 mutants, and somewhat less in the case of Y149F.

Participation of Tyr 149 and Ser 124 in Charge-Transfer Complexation. The near-UV absorption spectrum of epimerase reveals the presence of a charge-transfer band, which appears as a tail extending from 300 to 360 nm (*19*). Such bands are often observed in enzyme·NAD^+ complexes but have not often been structurally characterized (*37*). The close proximity between the nicotinamide ring of NAD^+ and the phenolic oxygen of Tyr 149 in epimerase (Figure 3) suggests that they may interact in charge-transfer complexation. That this is the case is strongly supported by the data in Figure 5, where the pH dependencies of charge-transfer intensities for the wild-type and mutant epimerases appear as plots of A_{320} against pH. The charge-transfer bands in the wild-type and

Ser 124 mutant epimerases decrease in intensity with decreasing pH. The pK_a values are 6.08 ± 0.10 for wild-type epimerase, 6.71 ± 0.06 for S124A, 6.86 ± 0.17 for S124V, and 6.28 ± 0.08 for S124T. The Y149F epimerase does not display a significant charge-transfer band. The simplest interpretation of these results is that the charge-transfer band arises from complexation between the phenolic oxygen of Tyr 149 and the nicotinamide ring of NAD^+ and is weakened in Y149F. The pH dependence indicates that the charge-transfer interaction is strongest between the phenolate form of tyrosine (Tyr 149−O^-) and NAD^+, and it is weakened by protonation of the side chain to Tyr 149−OH. The pH dependence indicates that the pK_a of Tyr 149 in wild-type epimerase is 6.08. Charge-transfer complexation also involves Ser 124 indirectly, presumably through hydrogen bond donation from its hydroxyl group to Tyr 149−O^-. That this is the case is indicated by the higher pK_a values for S124A and S124V, which would lack hydrogen bond stabilization from Ser 124. This interpretation is reinforced by the near normal pK_a for S124T, which presumably retains the capacity of the wild-type enzyme to donate a hydrogen bond to Tyr 149−O^-.

DISCUSSION

In considering the biochemical properties of specific mutant enzymes, it is important to know the structural consequences of the mutations. Substitutions of Ala, Thr, or Val for Ser at position 124 do not cause major structural changes, apart from the local differences that attend the substitutions themselves (*28*). Similarly, the only significant structural change upon replacing Tyr 149 with Phe is the loss of the phenolic oxygen (Figure 3a). Therefore, this discussion is based on the premise that the structures of the mutant epimerases are similar to that of wild-type enzyme except in the altered amino acid side chains.

Catalytic Functions of Tyr 149 and Ser 124. A major mechanistic issue in the action of epimerase has been the identification of a general acid−base catalyst that would facilitate hydride transfer from galactosyl or glucosyl C-4 substrates to nicotinamide C-4 of NAD^+. Chemical modification experiments in this laboratory have not been useful. For example, diethyl pyrocarbonate inactivates the enzyme rapidly, and UDP-phenol protects against inactivation. However, hydroxylamine does not reactivate the enzyme (*38*). Therefore, the group modified by diethyl pyrocarbonate could not have been histidine, and another modified amino acid could not be identified. Furthermore, two efforts to derivatize a general base at the active site by affinity labeling failed, both times because the affinity labeling agent reacted with NAD^+ at the active site and not with an amino acid (*39*, *40*).

The X-ray crystal structure of the abortive complex epimerase·NADH·UDP-Glc has drawn attention to Tyr 149 and Ser 124 as amino acids that interact directly with NAD^+ and UDP-Glc (*5*). The mechanistic roles of these amino acids could include general acid−base catalysis of hydride transfer from C-4 or/and orienting the pyranose ring through hydrogen bonding to the C-3-hydroxyl group. The present results implicate Tyr 149 as the principal driving force for general acid−base catalysis in the active site of epimerase. Among the mutated epimerases studied, Y149F is the most severely compromised kinetically, both as an epimerase and in the UMP-dependent reduction by glucose (Tables 2 and 3). Moreover, the pK_a of 6.08 for Tyr 149 correlates very well with the kinetically measured pK_a for the reduction of epimerase·NAD^+ by UDP-6-Glc, which is 6.1−6.2 after correction for the pH dependence of the deuterium kinetic isotope effect in the reaction of UDP-6-[1-^{2}H]Glc (*41*).

Scheme 2

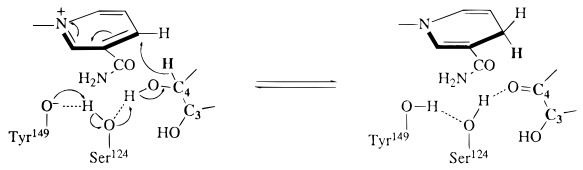

Ser 124 also participates in an important way in the chemical mechanism. Mutation of this residue to Ala decreases epimerase activity and UMP-dependent reactivity with glucose by factors of 2.9×10^3 and 3.7×10^2, respectively. However, S124A retains 3.6 times the epimerase activity of Y149F and is about 17 times as reactive in UMP-dependent reductive inactivation by glucose, so the role of Ser 124 appears to be secondary to that of Tyr 149.

The crystal stucture of the abortive complex (epimerase·NADH·UDP-Glc) shows the hydroxyl group of Ser 124 within 2.6 Å of the 4-hydroxyl group of glucose. The most obvious correlation of the kinetic, spectrophotometric, and X-ray structural facts is that both Tyr 149 and Ser 124 participate in general acid−base catalysis. Proton transfer is driven by Tyr 149 and mediated by Ser 124 as illustrated in Scheme 2. In this way, Tyr 149 provides the driving force for general acid−base catalysis and Ser 124 mediates catalysis by a proton relay mechanism. Inasmuch as the X-ray structures compared in Figure 3 are those of abortive complexes, in which the substrate and coenzyme are not in oxidation states that would exist in catalytically competent complexes, alternative possibilities may exist. The abortive complex can be regarded either as an analog of a Michaelis complex (epimerase·NAD^+·UDP-Glc) or as an analog of the central intermediate (epimerase·NADH·4-keto-Glc). In the case of the wild-type enzyme, the abortive complex is more similar to the central intermediate than to a Michaelis complex for the following reasons. First, the uridine nucleotide is more tightly bound in the abortive complex than in Michaelis complexes, and enhanced binding of uridine nucleotides is a characteristic property of the central intermediate (*42*). The tighter binding of UDP to epimerase·NADH compared with that to epimerase·NAD^+ has been attributed to the larger number of close contacts between the reduced enzyme and UDP (*5*). Second, in both the wild-type central complex and the abortive complex, the phenol ring of Tyr 149 and nicotinamide ring of NADH are both electrostatically neutral. In contrast, in the Michaelis complexes, the phenolate moiety of Tyr 149 forms a charge-transfer interaction with the positively charged nicotinamide ring of NAD^+.

Because the central complex is epimerase·NADH·UDP-4-keto-Glc, there can be no assurance that the hydrogen bonding observed for UDP-Glc in the abortive complex will be the same as that for UDP-4-keto-Glc. In particular, the 4-oxo group of UDP-4-keto-Glc is exclusively a hydrogen bond acceptor, whereas the 4-hydroxyl group of UDP-Glc can either donate or accept hydrogen bonds. This difference might perturb the hydrogen bonding network in the active

Scheme 3

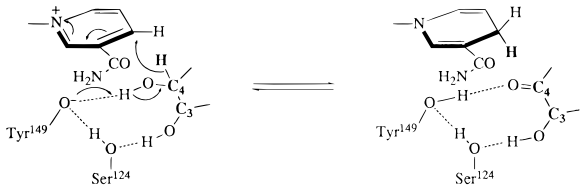

Scheme 4

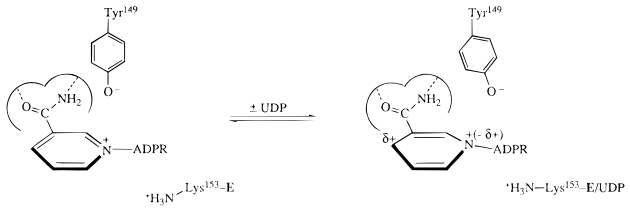

site. It is significant in this connection that the binding affinity of epimerase·NADH for UDP-4-keto-Glc is 100 times that for UDP-Glc (*42*), which suggests that binding of the hexopyranosyl ring may be perturbed in the abortive complex.

Until the structure of the catalytically functional central complex or that of a Michaelis complex such as epimerase·NAD^+·UDP-Glc is determined, the exact role of Ser 124 cannot be determined. For the present, two mechanisms of general acid−base catalysis should be considered, Scheme 2 above and one in which Tyr 149 acts directly on the 4-OH groups of the pyranosyl portions of substrates, with Ser 124 hydrogen bonded to Tyr 149 and perhaps also to substrate hydroxyl groups. Such a mechanism is illustrated in Scheme 3. A final distinction between these mechanisms would be provided by a structure for a Michaelis complex or the central intermediate (epimerase·NADH·UDP-4-keto-Glc).

Charge-Transfer Interaction and Uridine Nucleotide-Dependent Conformational Change. The value of pK_a for Tyr 149 (6.08) is 4 units lower than the corresponding value in aqueous solution (10.1). This difference corresponds to 5.5 kcal mol^{-1} of additional free energy of stabilization for the phenolate form that is provided by the microenvironment of the active site relative to an aqueous environment. Much of this stabilization can be attributed to the positive electrostatic field created by the nearby positive charges on the nicotinamide ring and Lys 153, which is hydrogen bonded to the 2′- and 3′-hydroxyl groups of the nicotinamide ribose moiety of NAD^+. The electrostatic field has been implicated in the uridine nucleotide-dependent conformational change and in its effect on the reactivity of NAD^+ (*17*, *43*). Mutation of Lys 153 to Met or Ala abolishes the UMP dependence of reductive inactivation by sodium cyanoborohydride. The positive electrostatic field would stabilize the phenolate form of Tyr 149 and thereby account for a low value of pK_a. However, Ser 124 also participates in stabilizing the phenolate form of Tyr 149, as shown by the fact that mutation to Ala or Val leads to higher values of the pK_a, 6.7 and 6.8, respectively. These differences correspond to about 1 kcal mol^{-1} of decreased stabilization in the mutants. Therefore, about 4.5 kcal mol^{-1} of stabilization may be attributed to the positive electrostatic field and the balance to Ser 124. Threonine in this position is slightly less stabilizing (pK_a = 6.28) than serine.

The charge-transfer interaction of Tyr 149 with NAD^+ has consequences for the chemical reactivity of NAD^+, as shown by the fact Y149F is more reactive with sodium cyanoborohydride than the wild-type epimerase, both in the presence and in the absence of UMP (Table 4). The phenolate of Tyr 149 attenuates the reactivity of NAD^+ by opposing the positive electrostatic field, which has been implicated in the enhanced reactivity of NAD^+ that is brought about by the uridine nucleotide-dependent conformational change (*17*, *43*). The uridine nucleotide-induced conformational change also alters the charge-transfer interaction, as shown by the fact that the charge-transfer band is bleached by UMP or UDP (*19*). Evidently, the conformational change alters the interactions of both Lys 153 and Tyr 149 with NAD^+. These changes have the following effects. The reactivity of NAD^+ is increased through an enhancement of the positive electrostatic field, and the charge-transfer interaction is perturbed, either through a change in the angular orientation of Tyr 149 relative to the nicotinamide ring or by an increase in the distance between them. These changes are given a conceptual framework in Scheme 4; however, the true nature of the conformational change and its effects on interactions of NAD^+ cannot be determined until the structure of the free enzyme becomes available.

Tyrosine as a General Acid−Base Catalyst in Short-Chain Dehydrogenase/Reductases. The tyrosine and serine residues in other short-chain dehydrogenase/reductases that correspond to Tyr 149 and Ser 124 of epimerase have been postulated to function in general acid−base catalysis on the basis of X-ray crystallographic structural models (*8*, *9*). Tyr 151 and Lys 155 have been shown to be important for activity in 15-hydroxyprostaglandin dehydrogenase through site-directed mutagenesis and kinetic studies (*44*), as have Tyr 179 and Lys 183 in 11β-hydroxysteroid dehydrogenase (*45*). The present work demonstrates the importance of Tyr 149 and Ser 124 in epimerase through X-ray crystallogrphic, kinetic, and spectrophotometric analysis of specific mutants. The importance of the corresponding Ser 138 in 15-hydroxyprostaglandin dehydrogenase has recently been proven through site-directed mutagenesis and kinetic analysis (*46*).

ACKNOWLEDGMENT

The authors acknowledge Dr. Barbara A. Swanson for her assistance in repairing sequence errors in the synthetic gene.

REFERENCES

1. Persson, B., Krook, M., and Jörnvall, H. (1995) in *Enzymology and Molecular Biology of Carbonyl Metabolism 5* (Weiner, H., et al., Eds.) pp 383−395, Plenum Press, New York.
2. Baker, M. E., and Blasco, R. (1992) *FEBS Lett. 301*, 89−93.
3. Holm, L., Sander, C., and Murzin, A. (1994) *Struct. Biol. 1*, 146−147.
4. Thoden, J. B., Frey, P. A., and Holden, H. M. (1996) *Biochemistry 35*, 2557−2566.
5. Thoden, J. B., Frey, P. A., and Holden, H. M. (1996) *Biochemistry 35*, 5137−5144.
6. Thoden, J. B., Frey, P. A., and Holden, H. M. (1996) *Protein Sci. 5*, 2149−2161.
7. Varughese, K. I., Skinner, M. M., Whiteley, J. M., Matthews, D., and Xuong, N. H. (1992) *Proc. Natl. Acad. Sci. U.S.A. 89*, 6080−6084.
8. Varughese, K. I., Xuong, N. H., Kiefer, P. M., Matthews, D. A., and Whiteley, J. M. (1994) *Proc. Natl. Acad. Sci. U.S.A. 91*, 5582−5586.

9. Tanaka, N., Nonaka, T., Yoshimoto, T., Tsuru, D., and Mitsui, Y. (1996a) *Biochemistry 35*, 7715−7730.
10. Tanaka, N., Nonaka, T., Nakanishi, M., Deyashiki, Y., Hara, A., and Mitsui, Y. (1996b) *Structure 4*, 33−45.
11. Ghosh, D., Weeks, C. M., Grochulski, P., Duax, W. L., Erman, M., Rimsay, R. l., and Orr, J. C. (1991) *Proc. Natl. Acad. Sci. U.S.A. 88*, 10064−10068.
12. Ghosh, D., Wawrzak, Z., Weeks, C. M., Duax, W. L., and Erman, M. (1994) *Structure 2*, 629−640.
13. Ghosh, D., Pletnev, V. A., Zhu, D. W., Wawrzak, Z., Duax, W. L., Pangborn, W., Labrie, F., and Lin, S. X. (1995) *Structure 3*, 503−513.
14. Azzi, A., Rehse, R. H., Zhu, D.-W., Campbell, R. L., Labrie, F., and Lin, S.-X. (1996) *Nat. Struct. Biol. 3*, 665−668.
15. Frey, P. A. (1987) in *Pyridine Nucleotide Coenzymes: Chemical, Biochemical, and Medical Aspects* (Dolphin, D., Poulson, R., and Avramovic, O., Eds.) pp 461−511, John Wiley & Sons, Inc., New York.
16. Thoden, J. B., Hegeman, A. D., Wesenberg, G., Chapeau, M. C., Frey, P. A., and Holden, H. M. (1997) *Biochemistry 36*, 6294−6304.
17. Swanson, B. A., and Frey, P. A. (1993) *Biochemistry 32*, 13231−13236.
18. Vanhooke, J. L., and Frey, P. A. (1994) *J. Biol. Chem. 269*, 31496−31504.
19. Liu, Y., Vanhooke, J. L., and Frey, P. A. (1996) *Biochemistry 35*, 7615−7620.
20. Maniatis, T., Fritsch, E. F., and Sambrook, J. (1982) *Molecular Cloning*, Cold Spring Harbor Laboratory Press, Plainview, NY.
21. Hattori, M., and Sakaki, R. Y. (1986) *Anal. Biochem. 152*, 232−238.
22. Sinha, N. D., Beirnat, J., McManus, J., and Koester, H. (1984) *Nucleic Acids Res. 12*, 4539−4557.
23. Smith, H. O. (1980) *Methods Enzymol. 65*, 371−380.
24. Richardson, C. C. (1971) in *Procedures in Nucleic Acids Research* (Canton, G. L., and Davies, D. R., Eds.) Vol. 2, pp 815−828, Harper and Row, New York.
25. Burns, D. M., and Beacham, I. R. (1983) *Anal. Biochem. 135*, 48−51.
26. Saiki, R. K., Gelfand, D. H., Stoffel, S., Scharf, S. J., Higuchi, R. Hori, G. T., Mullis, K. B., and Erlich, H. A. (1988) *Science 239*, 487−491.
27. Majumdar, A., and Adhya, S. (1987) *J. Biol. Chem. 262*, 13258−13262.
28. Thoden, J. B., Gulick, A. M., and Holden, H. M. (1997) *Biochemistry 36*, 10685−10695.
29. Sambrook, J., Fritsch, E. F., and Maniatis, T. (1989) *Molecular Cloning: A Laboratory Manual* (Nolan, C., Ed.) 2nd ed., Vol. 3, p A.3.
30. Tronrud, D. E., Ten Eyck, L. F., and Matthews, B. W. (1987) *Acta Crystallogr. A 43*, 489−501.
31. Kunkel, T. A., Roberts, J. D., and Zakour, R. A. (1987) *Methods Enzymol. 154*, 367−382.
32. Davis, J. E., Nolan, L. D., and Frey, P. A. (1974) *Biochim. Biophys. Acta 334*, 442−447.
33. Kalckar, H. M., Bertland, A. U., and Bugge, B. (1970) *Proc. Natl. Acad. Sci. U.S.A. 65*, 1113−1119.
34. Ketley, J. N., and Schellenberg, K. A. (1973) *Biochemistry 12*, 315−320.
35. Kang, U. G., Nolan, L. D., and Frey, P. A. (1975) *J. Biol. Chem. 250*, 7099−7105.
36. Konopka, J. M., Halkides, C. J., Vanhooke, J. L., Gorenstein, D. G., and Frey, P. A. (1989) *Biochemistry 28*, 2645−2654.
37. Rizzo, V., Pande, A., and Luisi, P. L. (1987) in *Pyridine Nucleotide Coenzymes* (Dolphin, D., Poulson, R., and Avramovic, O., Eds.) Vol. IIA, pp 99−161, Wiley and Sons, New York.
38. Flentke, G. R. (1988) Ph.D. Dissertation, University of Wisconsin−Madison, Madison, WI.
39. Wong, Y.-H., and Frey, P. A. (1979) *Biochemistry 18*, 5337−5341.
40. Flentke, G. R., and Frey, P. A. (1990) *Biochemistry 29*, 2430−2436.
41. Arabshahi, A., Flentke, G. R., and Frey, P. A. (1988) *J. Biol. Chem. 263*, 2638−2643.
42. Wong, S. S., and Frey, P. A. (1977) *Biochemistry 16*, 298−305.
43. Burke, J. R., and Frey, P. A. (1993) *Biochemistry 32*, 13220−13230.
44. Ensor, C. M., and Tai, H. H. (1994) *Biochim. Biophys. Acta 1208*, 151−156.
45. Obeid, J., and White, P. C. (1992) *Biochem. Biophys. Res. Commun. 188*, 222−227.
46. Ensor, C. M., and Tai, H. H. (1996) *Biochem. Biophys. Res. Commun. 220*, 330−333.

BI970430A